Electropolymerization of Polypyrrole and Polypyrrole-ZnO Nanocomposites on Mild Steel and Its Corrosion Protection Performance

M. G. Hosseini,[1] R. Bagheri,[1] R. Najjar[2]

[1]*Department of Physical Chemistry, Electrochemistry Research Laboratory University of Tabriz, Tabriz, Iran*
[2]*Department of Organic Chemistry, Polymer Research Laboratory, University of Tabriz, Tabriz, Iran*

Received 10 March 2010; accepted 27 November 2010
DOI 10.1002/app.33952
Published online 6 April 2011 in Wiley Online Library (wileyonlinelibrary.com).

ABSTRACT: Polypyrrole (PPy) and Polypyrrole-ZnO (PPy-ZnO) nanocomposites were electrodeposited on mild steel and its corrosion protection ability was studied by Tafel and Impedance techniques in 3.5% NaCl solution. Pure Polypyrrole film was not found to protect the mild steel perfectly but the coating with nano-sized ZnO (PPy-ZnO) has dramatically increased the corrosion resistance of mild steel. Electrochemical Impedance Spectroscopy (EIS) measurements indicated that the coating resistance (R_{coat}) and corrosion resistance (R_{corr}) values for the PPy-ZnO nanocomposite coating was much higher than that of pure PPy coated electrode. © 2011 Wiley Periodicals, Inc. J Appl Polym Sci 121: 3159–3166, 2011

Key words: conducting polymers; nanocomposites; electrochemistry; corrosion; polypyrrole

INTRODUCTION

Conducting polymers due to their nontoxic, environmentally friendly, high stability and ease of synthesis, are the most promising coatings for corrosion protection of industrial metals. Among various conducting polymers, polypyrrole has been extensively investigated because of its attractive properties from the practical point of view, e.g., the relatively good environmental stability, the high conductivity, and the ease of preparation either by chemical or by electrochemical polymerization.[1–8] A new method for the synthesis of conducting polypyrroles (PPy), based on chemical and combined electrochemical-chemical oxidation of pyrrole monomers.[9] Simultaneous formation and deposition of electrically conductive polymers are possible by electrochemical polymerization technique. Using this technique, controlling the thickness and uniformity of coatings is possible and practical. In addition, nontoxic and nonvolatile chemicals for polymer coating, allows this method an environmental friendly process.[10]

Application of PPy coatings for corrosion protection of metals and alloys is however subjected to some limitations. The first, charges stored in the polymer layer can be irreversibly consumed during the system's redox reactions. Consequently, quality of the protection with polymer coatings may be lost with time. Also, porosity and ion exchanges of PPy coatings might be disadvantageous, particularly when it comes to localized corrosion caused by small and aggressive anions. Therefore, interests have been focused on the use of conducting polymers as copolymers,[9–13] composites,[14–16] nanocomposites[17–20] or bilayers.[21,22] In this reasearch, following our previous investigations,[23–26] first, the possibility of electrochemical synthesis of PPy-ZnO nanocomposite films on mild steel electrode was studied using Fourier Transform Infrared (FT-IR) spectroscopy and Scanning Electron Microscopy (SEM) techniques then, its protective performance against corrosion in 3.5% NaCl solution was evaluated using Electrochemical Impedance Spectroscopy (EIS).

EXPERIMENTAL

Materials

Pyrrole and oxalic acid were purchased from Merck. Dodecylbenzene sulfonic acid (DBSA) as acid dopant was supplied by Fluka. Pyrrole was purified by distillation under vacuum just before use and all the aqueous solutions were prepared with distilled water. ZnO nanorods were prepared according to

Correspondence to: M. G. Hosseini (mg-hosseini@tabrizu.ac.ir).

Contract grant sponsor: Vice Chancellor in Charge of Research of Tabriz University and Research of Iranian Nanotechnology Society.

Journal of Applied Polymer Science, Vol. 121, 3159–3166 (2011)

the literature with some modification of the reaction condition.[27] Briefly, a 50 mL of 1 mol/L $ZnSO_4$ solution was placed in a three-necked flask and vigorously stirred at 70°C. Zinc sulfate was adopted as the source material for zinc species. For acceleration of the formation of ZnO particles, while vigorous stirring 50 mL of 1 mol/L Na_2CO_3 solution containing certain amount of sodium oleate was added dropwise to the $ZnSO_4$ solution and afterwards 50 mL of NaOH solution with the same concentration was added to the mixture. After the addition is complete, the reaction mixture is stirred for another 30 min. Subsequently, the resulting slurry was filtered and washed several times to remove excessive ions by distilled water and ethanol. Finally, ZnO nanorods were obtained after drying an oven at 120°C for 20 h.

Electropolymeristion of PPy and PPy-ZnO nanocomposite on mild steel

For preparation of PPy-ZnO nanocomposites with 10 wt % ZnO loading, first, 0.13 g ZnO nanorod powder was introduced into the 200 mL oxalic acid (0.1*M*) and 1 mL dodecylebenzensulfonic acid under magnetic stirring at room temperature and was stirred for two hours. Then, pyrrole monomer (1.3 g) was added to the reaction mixture and stirred for another one hour. The electropolymerization was performed in a one-compartment three electrode cell at room temperature (25°C). For all electrochemical studies, the reference electrode was a saturated calomel electrode (SCE). The electrolyte solution was purged with pure nitrogen during the each experiment. A mild steel specimen embedded in resin with an exposed surface area of 1 cm^2 was used as working electrode and platinum gauze as counter electrode.

Before each experiment, the working electrodes were carefully polished with sequence emery papers of various grades (220–3000 grit). Electrochemical polymerization was carried out under galvanostatic conditions at room temperature. A Potentiostat/Galvanostat (PAR EG and G model 2263) was used in the electrochemical experiments. The applied current densities were 1, 2, and 3 mA cm^{-2}. The optimal coating with high corrosion resistance was obtained using 2mA cm^{-2} current density with 1 h deposition time. Therefore, this value of current density was applied for the preparation of coatings on mild steel. After each experiment, the coated mild steel sheet was rinsed with water, dried and used for corrosion experiments.

Characterization of electropolymerized film

After preparation of the films (PPy and PPy-ZnO nanocomposite) on mild steel, the film was scrabbed and mixed with KBr to make the FT-IR spectra. FT-IR spectra were recorded as KBr dispersions by a Bruker Tensor 27 instrument in the 4000–400 cm^{-1}. The morphology of the PPy and PPy-ZnO nanocomposite coatings were characterized by a Philips XL30 scanning electron microscope (SEM).

Corrosion study

The protection properties of coatings were investigated in 3.5% NaCl solution by open circuit potential (OCP), Tafel polarization and EIS techniques. In EIS measurements the AC frequency range extended from 100 kHz to 10 mHz. Then the real and imaginary components of the impedance spectroscopy in the complex plane were analyzed by using the ZView (II) software to estimate the parameters of the equivalent electrical circuits.

Tafel polarization measurements were carried out on a corrosion protective PPy or PPy-ZnO nanocomposite film obtained at optimum current density (2 mA cm^{-2}) at a sweep rate of 0.5 mV s^{-1}.

RESULTS AND DISCUSSION

Galvanostatic deposition

In the case of mild steel, anodic or chemical oxidation is accompanied by dissolution of the metal. The oxidation potential of most monomers is in the region of metal dissolution. The metal is able to retard or to inhibit the oxidation of the monomer and thus the formation of an adherent polymer film on that. Therefore, the mild steel surface must be pretreated to avoid strong corrosion parallel to the film formation. Figure 1 shows the potential versus time curves for electrodeposition of PPy and PPy-ZnO nanocomposite coating on to the mild steel at a current density of 2 mA cm^{-2}. The induction period at negative potentials (region a in Fig. 1) is attributed to an active dissolution of the iron at negative potentials for 8 and 20 min for PPy-ZnO nanocomposite and pure PPy coatings, respectively, where the potential shifts into the positive direction due to the precipitation of Fe (II) oxalate (region b in Fig. 1).

Polypyrrole (black and adherent deposit) was electrodeposited at the positive potential plateau (600 mV versus SCE) (region c in Fig. 1).

Characterization

Figure 2(a) shows the X-ray diffraction patterns of ZnO and indicates that the ZnO nanorod was synthesized. Grasset et al. have calculated the average crystal size from the width of each diffraction peak. X-ray diffraction is used to determine the

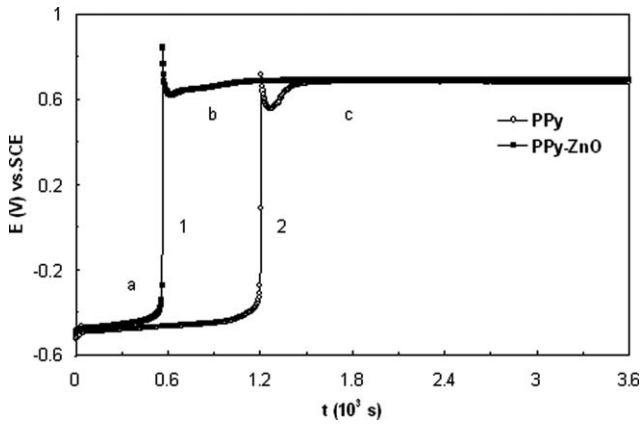

Figure 1 Potential versus time curves for the galvanostatic electrodeposition of: (1) PPy-ZnO nanocomposite and (2) pure PPy on mild steel from aqueous electrolyte (0.1*M* pyrrole, 0.1*M* $H_2C_2O_4$) at 2 mA cm^{-2}.

degree of crystallization of the nanoparticles. The Scherrer formula estimates particle size by measuring the crystal diffraction line broadening that is directly related to the crystal spacing and size.[28] Figure 2(b) shows the SEM image of ZnO as nanorod.

The FTIR spectra of ZnO nanorod, PPy, and PPy-ZnO nanocomposite coatings on mild steel are

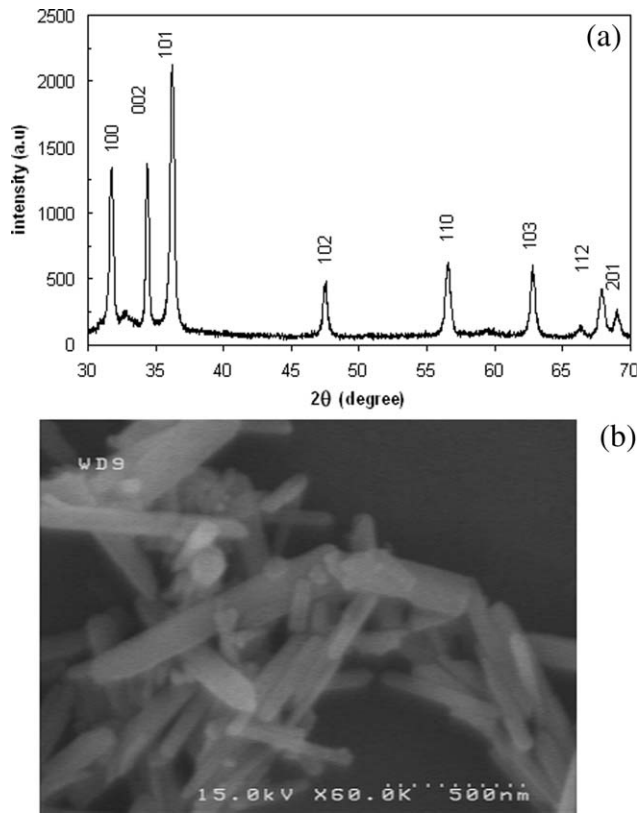

Figure 2 (a) XRD pattern and (b) SEM images of ZnO nanorods.

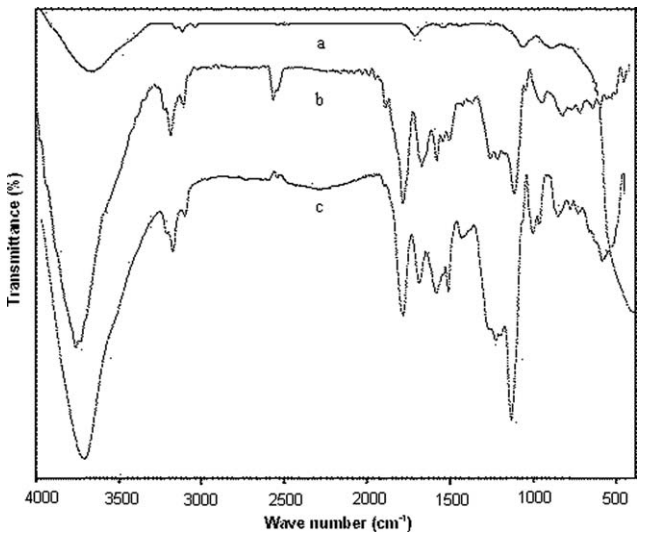

Figure 3 FT-IR spectra of: (a) ZnO nanorod; (b) PPy; and (c) PPy-ZnO nanocomposites.

shown in Figure 3. The band at 505 cm^{-1} is assigned to Zn-O bond. The peak around 1640 could be attributed to O—H bond. The peaks at 1537 cm^{-1} (C=C stretching), 1034 cm^{-1} (C—H vibration) and 1292 cm^{-1} (C—N stretching) are the characteristic adsorbtion peaks of PPy.[29]

SEM images allowed for a closer look at the morphology of the electropolymerized coatings of PPy and PPy-ZnO nanocomposite. Figure 4(a,b) compares the SEM images of pure PPy [Fig. 4(a)] and PPy-ZnO nanocomposite [Fig. 4(b)] coatings with magnification of 5000 times. The cauliflower-like structure of PPy coating[11,30] is well distinguishable from the nanocomposite coating where homogeneity of surface is much more expressed. As can be seen, the pure PPy coating has a completely different morphology compared with PPy-ZnO nanocomposite coating. The PPy has a bulky and porous appearance, which paves more pathways for electrolyte to reach the metal surface under the coating. But in the case of nanocomposite coating the surface is homogen and dense. In the presence of ZnO nanorods with the formation of nanocomposite the surface morphology changes a fine-grained structure. SEM images of nanocomposite with magnification of 5000 and 30,000 times were shown in Figure 4(b).

The expected role of the nano particles is to increase the barrier effect of the polymer matrix, improving its protecting properties. The excellent anticorrosion protection is attributed to the size and shape of nanorod, which has the small size and large aspect ratio. For the small particles, free space between the particles and polymer is far lesser than that of larger particles. Thus electrolyte is harder to penetrate through the pores in coating

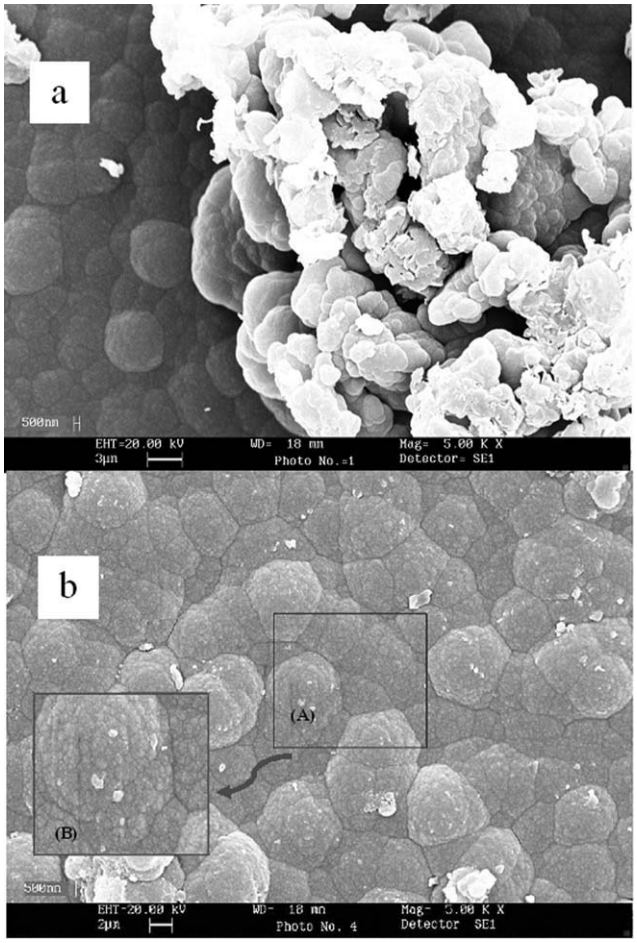

Figure 4 SEM images of: (a) PPy with magnification of 5000 times, (b) PPy-ZnO nanocomposite coating on mild steel with magnification of 5000 and 30,000 times.

film with addition of nano pigment. In addition due to longer diffusion path in nanocomposite costing, the water and ions need more time to arrive at the substrate.

Corrosion tests

Open circuit potential curves

The corrosion performance of mild steel electrode coated with PPy or PPy-ZnO nanocomposite films were investigated in 3.5% NaCl solution.

The E_{ocp} values measured for PPy and PPy/ZnO coated electrodes after various immersion times were plotted against time in Figure 5. The initial values measured for PPy and PPy/ZnO electrodes were −200 and 150 mV, respectively. However, with initiation of the up taking process these values were started to decrease and after 5 h, the E_{ocp} value of PPy electrode was reached to −600 mV. This implies that significant amounts of electrolyte solution has passed through the pores in coating and reached to the surface of underlying metal, causing the start of corrosion process. On the other hand, the E_{OCP} values recorded for PPy-ZnO coating were observed to shift towards a less negative value with time, and E_{OCP} was measured almost −100 mV after 5 h of exposure time to corrosive solution. Therefore, it can be concluded that this nanocomposite coating was able to keep its excellent barrier property during this period and there was no evidence for notable corrosion of underlying metal.

Polarization curves

Polarization measurements have been performed for evaluation of the protective properties of coatings. Tafel polarization plots for PPy-ZnO coatings in different current densities (1–3 mA cm^{-1}) exhibited high protection of mild steel at the current density of 2 mA cm^{-1}. The plots in Figure 6(a) indicate that after 5 h submerging in corrosive solution, corrosion potential of coatings in current density of 2 mA cm^{-1} is in more positive potentials than the other current densities.

As complementary experiments, the Tafel polarization curves [Fig. 6(b)] for two different electrodes (coated with PPy and PPy-ZnO) in the corrosive solution were plotted. Information on the corrosion parameters (i_{corr}, E_{corr}, and R_p) obtained by the Tafel extrapolation method are given in Table I.

Tafel results show that the introduction of the ZnO nanorods in the PPy coating led to the increase in R_p value compared to the R_p value of the pure PPy-coated electrode. Also, corrosion current (i_{corr} = 92.72 mA cm^{-2}) value for PPy coating is higher than that of PPy-ZnO coating (i_{corr} = 8.45 mA cm^{-2}). A nobler value of (E_{corr} = −95.96 mV) indicates that the PPy-ZnO nanocomposite coated electrode shows the highest corrosion protection properties.

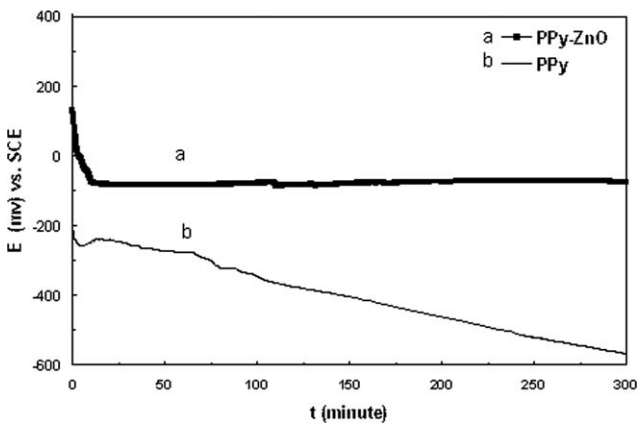

Figure 5 The variation of E_{corr} values with increasing immersion time in 3.5% NaCl solution for: (a) PPy-ZnO nanocomposite and (b) PPy coating.

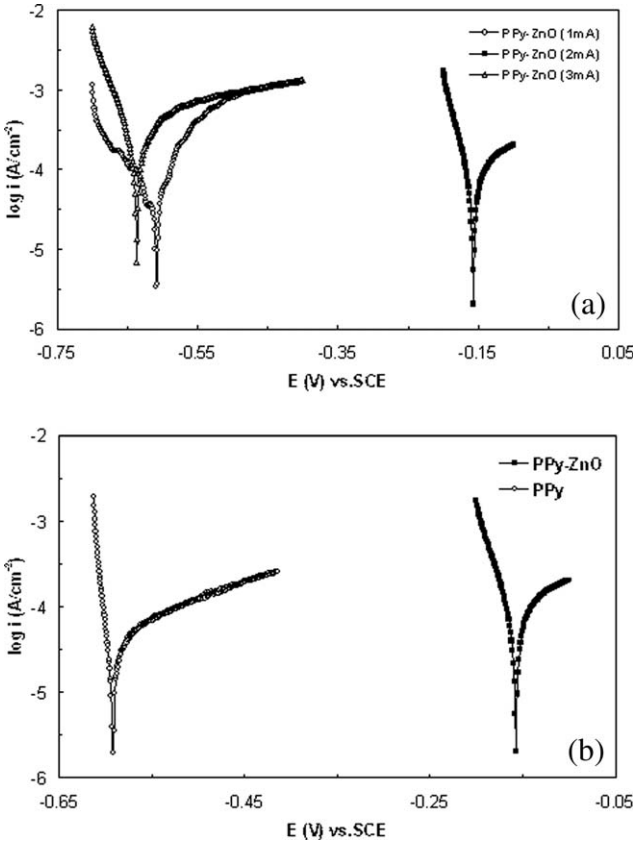

Figure 6 Tafel plot of (a) PPy-ZnO nanocomposite coated electrodes at different current densities (1, 2, 3 mA cm^{-2}) and (b) PPy and PPy-ZnO nanocomposite coatings at current density of 2 mA cm^{-2} after 5 h of submerging in 3.5% NaCl solution.

Electrochemical impedance spectroscopy

Electrochemical impedance spectroscopy is a technique which allows for evaluation of the wide variety of coating properties. Figure 7(a) illustrates the Nyquist diagrams recorded for PPy and PPy-ZnO nanocomposite coatings after 10, 60, 180, and 300 min exposure time in 3.5% NaCl solution. Equivalent circuit model appropriate for the Nyquist plots was used to correlate the impedance with capacitance and resistance of the film. For all coated mild steel electrodes, a physical model made up of two semicircles (or two time constants) that give a good fit to the experimental data. The semicircles appearing at high and middle frequencies are due to the reactions taking place at the coating/solution and metal/polymer interfaces, respectively. The electrical equivalent circuit which was used for fitting of the EIS data is depicted in Figure 7(b). In this equivalent circuit model, R_s is solution resistance, CPE (dl) represents the constant phase element for double layer and R_{corr} is the charge transfer resistance. The constant phase element for coating is indicated by CPE (coat).

The calculated values for coating parameters by ZView (II) software are given in Table II. The R_{coat} and R_{corr} values obtained for PPy-ZnO electrodes are relatively high with respect to pure PPy samples. These increases are related to the decrease of charge transfer rate between the metal and the solution. The charge transfer reactions are known to take place at the metal/polymer interfaces. Consequently the high R_{corr} values of PPy-ZnO electrodes can be explained by the effective barrier behavior of nanocomposite film. Also, the maintenance of passive layer formed prior to electropolymerization process, may be effective on this increase.[2] Comparison between PPy and PPy-ZnO coatings indicates that the charge transfer resistance and R_{coat} values are higher for PPy-ZnO coating. This excellent anticorrosion property is attributed to the size and shape of nanorod ZnO, which has the large aspect ratio.

The time dependence of coating resistance, R_{coat}, is given in Table II. It is seen clearly that for both coatings the coating resistances always decrease with increasing immersion time at the first 1–2 h, and then attains an approximately constant. Furthermore, it can be found that although the initial value of coating resistance for the PPy and PPy-ZnO coatings are close to each other, the resistance of the PPy coating decreases sharply and becomes much lower than that of the PPy-ZnO coating.

According to the following reasons, it is supposed that the protection life-time of the PPy-ZnO nanocomposite coating is longer than that of the pure PPy coating: (a) the existence of ZnO nanorods, to some extent increase the tortuosity of diffusion pathway of corrosion specimen. (b) PPy-ZnO coating is more compact compared with the PPy coating, which is also confirmed by the charge transfer resistance, R_{corr} (Table II). The decrease in R_{corr} for this coating corresponds to time required for electrolyte to reach the metal surface and to start corrosion process on the substrate. Higher value of R_{corr} obtained

TABLE I
Corrosion Parameters for PPy-ZnO and PPy Coatings on Mild Steel in 3.5 % NaCl Solution

	R_p (Ω cm^2)	E ($I = 0$) (mV vs. SCE)	I_{corr} (Ω cm^2)	β_c (mV/Decade)	β_a (mV/decade)
PPy-ZnO	2816.225	−95.966	8.453	85.814	94.469
Ppy	234.463	−575.45	92.72	11.104	33.035

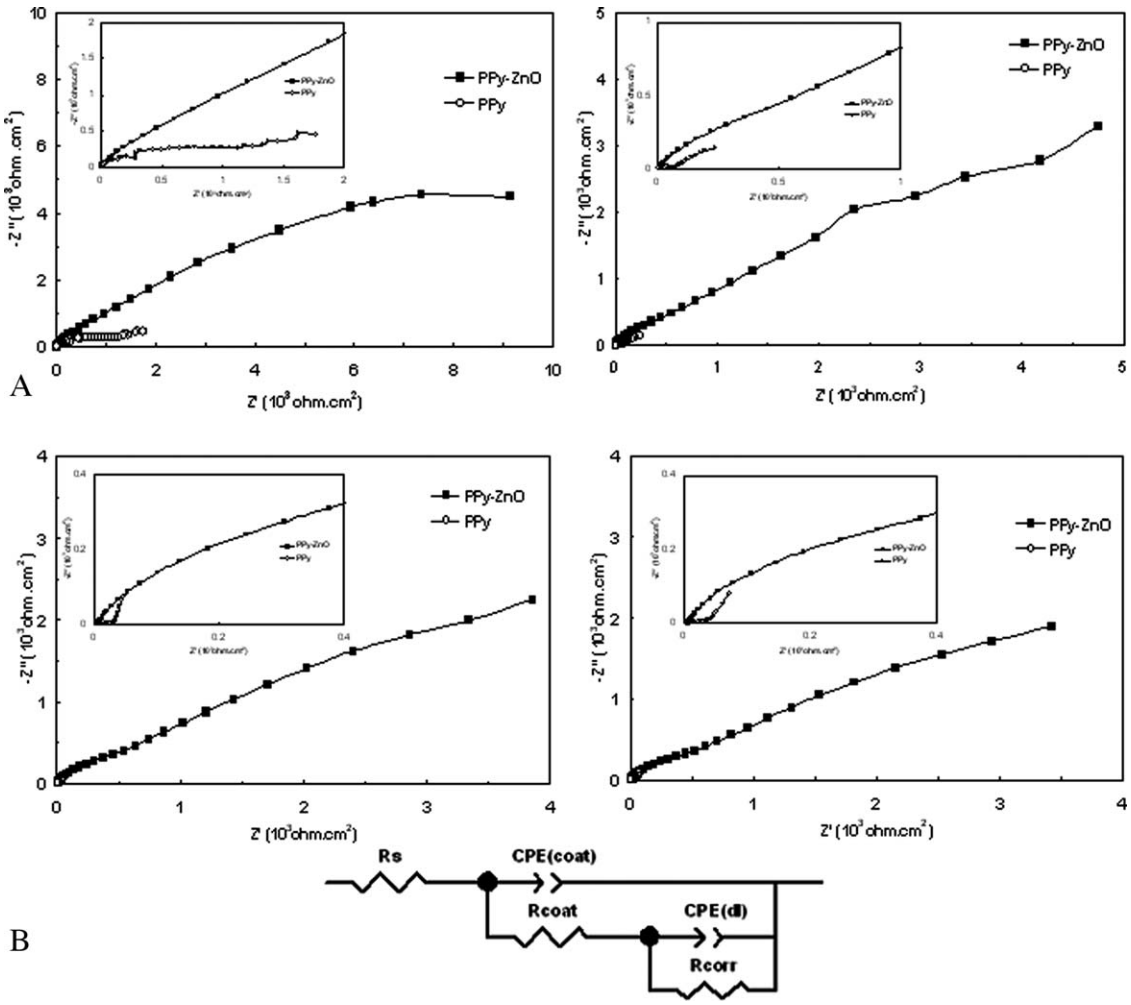

Figure 7 (a) The Nyquist plots of PPy and PPy-ZnO coatings after; (a) 10 min, (b) 1 h, (c) 3 h, (d) 5 h submerging in 3.5% NaCl solution. (b) Electrical circuit model to interpret the response of the PPy and PPy-ZnO coatings interface in EIS.

for PPy-ZnO nanocomposite coated mild steel with respect to PPy coated mild steel again points to its better corrosion protection properties. The comparison between the capacitance of PPy and PPy-ZnO coatings in Figure 8, indicate that unlike the PPy coating, the capacitance of PPy-ZnO coating decreasing with immersion time.

A constant phase element is an equivalent electrical circuit component that models the behavior of a layer, that is an imperfect capacitor. CPE is described by two parameters Y and n according to the equation: $Z_{CPE}(Y, n) = 1/Y\,(j\omega)^n$ where Y is the CPE-constant, j the imaginary unit, n the CPE power ($0 \leq n \leq 1$), and ω is the angular frequency ($\omega =$

TABLE II
Impedance Data Obtained by Simulation of Figure 8 by ZView (II) Software

	Time (min)	R_s (Ω cm^2)	R_{coat} (Ω cm^2)	$Y_0 \times 10^5$ (Ω^{-1} cm^{-2}) Coat	n_1 Coating	Capacity (μF)	$Y_0 \times 10^5$ (Ω^{-1} cm^{-2}) Metal	n_2 Metal	R_{corr} (Ωcm^2)
Mild steel/PPy	10	4.89	162.4	1.57	0.77	2.66	55.13	0.32	2209
	60	4.99	55.3	2.36	0.78	3.4	1482	0.48	2095
	180	5.99	19.17	20.08	0.67	12.95	9629	0.71	1123
	300	6.33	12.53	16.72	0.78	29.84	3400	0.4	670
Mild steel/Py/ZnO	10	6.16	950.8	12.8	0.77	68.23	33	0.53	18881
	60	6.66	425.4	8.71	0.8	38.33	55	0.49	17470
	180	6.15	368.1	7.65	0.81	32.45	65	0.46	15930
	300	6.4	352.2	7.28	0.81	30.14	74	0.46	13427

$2\Pi f$, f is the frequency). For $n = 1$ the CPE is a pure capacitance. For a capacitance element the deviation of the exponent n from unity is due to the heterogeneousness effect.

CPE (Y, n) in Table II represents the constant phase element for the coating, where Y and n are the parameters of the CPE.

The capacitance of coating (C_c) was calculated from the following formula:

$$C_c = (Y_0 \times R)^{(1/n)}/R$$

where R is the coating resistance (R_{coat}).

Also, the water uptake of coatings was calculated from the following formula.[22]

$$\text{water} - \text{uptake}(\%) = \frac{\left(\log C_c(t)/\log C_c(0)\right)}{\log(80)} \times 100$$

where C_c (t) is the coating capacitance at time (t) and C_c (0) the initial coating capacitance.

On the other hand, water uptake is a common parameter used for predicting anticorrosion performances of organic coatings.[22] The water uptake values were calculated and plotted as a function of time in Figure 9. The pure PPy-coated electrode, in the absence of ZnO nanorod, absorbs a large amount of water and water uptake increases quickly, while the water uptake of PPy-ZnO nanocomposite coating has a decreasing trend with immersion time.

The increase in C_c for pure PPy coating with time denoted the entry of electrolyte into the coating.[17] But, in the case of PPy-ZnO nanocomposite coating, a decreasing trend with time is observed for C_c, which is attributed to the denser structure of the PPy-ZnO coating compared to the pure PPy coating. Therefore, the electrochemical reactions occur in the bottom of the pores, and the corrosion products can fill the pores and causing to the depletion of the water, consequently to the lower water uptake values.

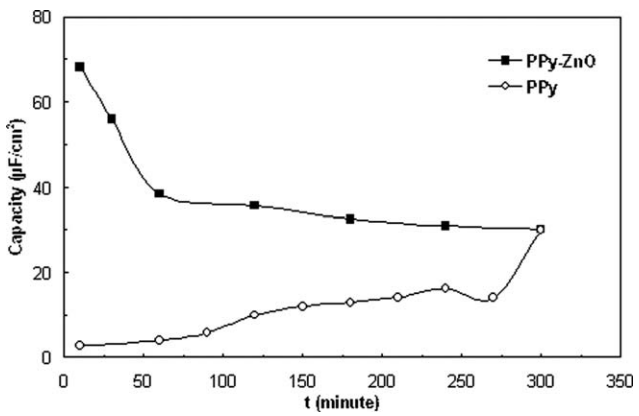

Figure 8 The time dependence of C_{coat} for PPy and PPy-ZnO nanocomposite coatings on mild steel in 3.5% NaCl solution.

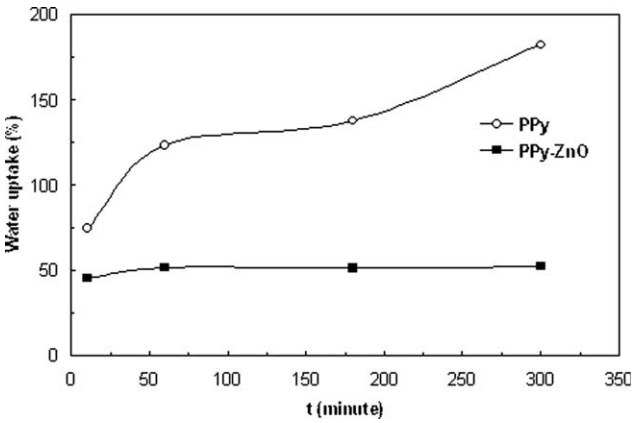

Figure 9 The time dependence of Water Uptake (%) for PPy and PPy-ZnO nanocomposite coatings on mild steel in 3.5% NaCl solution.

CONCLUSION

In this work, the synthesis of ZnO nanoroads was proved by XRD pattern. Also a procedure for the electrodeposition of PPy on mild steel using ZnO nanorods has been described. A strongly adherent polypyrrole film was obtained by galvanostatic electrodeposition on mild steel, with a current density of 2 mA cm^{-2} in 0.1M oxalic acid and 0.1M pyrrole solution.

SEM images demonstrate that PPy-ZnO coating has merit morphological characteristic to protect the mild steel against corrosive media. Also the data obtained from the OCP show that the PPy-ZnO nanocomposite polymer film shifts the electrode potential towards more positive potentials and the parameters obtained from Tafel test point out that the PPy-ZnO coating improves anticorrosion properties of PPy coating. EIS measurements illustrate that the best corrosion protection properties for investigated coatings in this work, are obtained when ZnO nanorods were incorporated in PPy coating. Incorporation of nanosized ZnO (10 wt % relative to PPy) into the polypyrrole matrix resulted in an increase in corrosion resistance of PPy coating. These have been attributed to the morphology of nanocomposite in which the particle size and specific surface area are modified with the incorporation of nanorods.

References

1. Hammache, H.; Makhloufi, L.; Saidani, B. Corros Sci 2003, 45, 2031.
2. Tan, C. K.; Blackwood, D. J. Corros Sci 2003, 45, 545.
3. Hosseini, M. G.; Sabouri, M.; Shahrabi, T. Mater Corros 2007, 57, 407.

4. Hosseini, M. G.; Sabouri, M.; Shahrabi, T. Prog Organ Coat 2007, 60, 178.
5. Sabouri, M.; Sharabi, T.; Hosseini, M. G. R. J Electrochem 2007, 43, 1390.
6. Tuken, T. Surface Coat Technol 2006, 200, 4713.
7. Grgur, B. N.; Zivkovic, P.; Gvozdenovic, M. M. Prog Organ Coat 2006, 56, 240.
8. Anuar, K.; Murali, S.; Fariz, A.; Mahmud Ekramul, H. N. M. Mater Sci 2004, 10, 255.
9. Yeh, J. M.; Chin, C. P.; Chang, S. J Appl Polym Sci 2003, 88, 3264.
10. Ashrafi, A.; Gholzar, M. A.; Mallakpour, S. Synthetic Metals 2006, 156, 1280.
11. Ocon, P.; Cristobal, A. B.; Herrasti, P.; Fatas, E. Corros Sci 2005, 47, 649.
12. Boukerma, K.; Piquemal, J. Y.; Chehimi, M. M.; Mravcakova, M.; Omastova, M.; Beaunier, P. Polymer 2006, 47, 569.
13. Rodriguez, J.; Grande, H.; Otero, TF. Chichester 1997, 2, 68.
14. Armes, SP. Handbook of Conducting Polymers, 2nd ed.; Marcel Dekker: New York, 1998, p 423.
15. Omastova, M.; Pionteck, J.; Kosina, S. In Electronic and Optical Properties of Conjugated Molecular Systems in Condensed Phases; Hotta S, Ed.; Research Signpost: Kerala, India, p 86–153.
16. Castro, E. G.; Zarbin, A. J. G.; Galembeck, A. J. Non-Cryst Solids 2005, 351, 3704.
17. Visy, C.; Bencsik, G.; Nemeth, Z.; Vertes, A. Electrochimica Acta 2008, 53, 3942.
18. Sathiyanarayanan, S.; Muthkrishnan, S.; Venkatachari, G. Electrochimica Acta 2006, 51, 6313.
19. Popov, B. N.; Alwohaibi, M. A.; White, R. E. J Electrochem Soc 1993, 140, 947.
20. Omastova, M.; Trchova, M.; Kovarova, J.; Stejskal, J. Synthetic Metals 2003, 138, 447.
21. Patil, R. C.; Radhakrishnan, S. Prog Organ Coat 2006, 57, 332.
22. Yang, H.; van Ooij, W. J. Prog Organ Coat 2004, 50, 149.
23. Hosseini, M. G.; Sabouri, M.; Shahrabi, T. J Appl Polym Sci 2008, 110, 2733.
24. Sabouri, M.; Shahrabi, T.; Hosseini, M. G. Mater Corros 2008, 59, 814.
25. Sabouri, M.; Shahrabi, T.; Faridi, H. R.; Hosseini, M. G. Progr Organ Coat 2009, 64, 249.
26. Hosseini, M. G.; Ragibi-Brojeni, M.; Ahadzadeh, I.; Najjar, R.; Seyed Dorraji, M. S. Prog Organ Coat 2009, 66, 321.
27. Lanqin, T.; Bing, Z.; Yumei, T.; Hari, B.; Yan, P.; Suxia, R.; Yi, W.; Xiaotang, L.; Minggang, L.; Zichen, W. Colloids Surfaces A Physicochem Eng Aspects 2007, 296, 92.
28. Grasset, F.; Saito, N.; Li, D.; Park, D.; Sakaguchi, I.; Ohashi, N.; Haneda, H.; Roisnel, T.; Mornet, S.; Duguet, E. J Alloy Compd 2003, 360, 298.
29. Kim, J. W.; Liu, F.; Choi, H. J.; Hong, S. H.; Joo, J. Polymer 2003, 44, 289.
30. Ferreira, C. A.; Domenech S. C., Lacaze, P. C. J Appl Electrochem 2001, 31, 49.